Relativistic Parametrization of the Self-Consistent-Charge Density-Functional Tight-Binding Method. 1. Atomic Wave Functions and Energies†

Henryk A. Witek*

Department of Applied Chemistry and Institute of Molecular Science, National Chiao Tung University, Hsinchu 30010, Taiwan

Christof Köhler and Thomas Frauenheim

Bremen Center for Computational Materials Science, Bremen University, 28359 Bremen, Germany

Keiji Morokuma

Fukui Institute for Fundamental Chemistry, Kyoto University, Kyoto 606-8103, Japan

Marcus Elstner

Institute for Physical and Theoretical Chemistry, Technical University, 38106 Braunschweig, Germany

Received: January 30, 2007; In Final Form: May 6, 2007

A detailed treatment of a confined relativistic atom, needed as an initial step for the parametrization of the self-consistent-charge density-functional tight-binding method, is presented and discussed. The required one-component quantities, i.e., orbital energies, orbital wave functions, and Hubbard parameters, are obtained by weighted averaging of the corresponding numbers determined for the atomic spinors. The wave function and density confinement is achieved by introducing the Woods−Saxon potential in the atomic four-component Dirac−Kohn−Sham problem. The effect of the additional confining potential on energy eigenvalues and the shape of atomic wave functions and densities is discussed and numerical examples are presented for the valence spinors of carbon, germanium, and lead.

I. Introduction

The growing importance of nanotechnology and biomolecular engineering has shifted the center of interest in many disciplines of molecular science from small and medium-size molecules to very large, extended atomic systems. This statement is especially true about theoretical branches of physics and chemistry. Until recently, usual systems studied by theoretical chemists using ab initio methods contained up to about 100 atoms due to the limitations of available computing resources. Dynamical development of computer technology allowed for shifting this limit to a few hundred atoms. Another way of enlarging the size of the system under study is a systematic and well-tested approximation scheme, where the usually very involved computational algorithms are replaced by simpler theories with lower computational complexity. These simplified approaches usually give lower accuracy of the final results, but in many situations are able to provide qualitative—and often also quantitative—answers to many interesting physical and chemical problems that would be intractable otherwise.

One of the first attempts to treat extended systems that contain a large number of atoms was the tight-binding (TB) technique of Slater and Koster.[1] A similar approach was adopted later by Seifert and his co-workers, who discussed the possibility of using density functional theory (DFT)[2−4] for parametrization of their version of the two-center TB method.[5−8] We refer to this approach and approaches derived from it as density-functional-based tight-binding (DFTB) methods. A strict theoretical interpretation of this type of TB techniques as an approximate, noniterative density functional theory was given at about the same time.[9,10] To extend the transferability of DFTB to various systems and to describe better the charge reorganization in polar molecules, Elstner and his co-workers introduced a self-consistent correction in the DFTB formalism. The resulting technique,[11] known as self-consistent-charge density-functional-based tight-binding (SCC−DFTB) method, uses iteratively determined induced atomic Mulliken charges as a descriptor of electron reorganization in a molecule. This extension allowed for the quality of total energies, band structures, geometries,[12] and vibrational frequencies[13−15] to be improved in comparison with the standard DFTB approach. Recently, a spin-polarization formalism was presented that enables high-spin open-shell molecular systems to be studied using SCC−DFTB.[16,17]

The SCC−DFTB method fulfills most of the requirements of a fast and reliable semiempirical computational technique. It considers explicitly only valence electrons and, therefore, allows for a substantially larger system size when compared to standard all-electron ab initio approaches. It has well-defined theoretical foundations; the approximations introduced in its derivation have been extensively analyzed and tested. The accuracy of the SCC−DFTB method is rather striking in comparison with other related approaches; reaction energies and molecular geometries determined with SCC−DFTB are often only slightly worse than those obtained from DFT calculations.[12]

† Part of the "DFTB Special Section".

* To whom correspondence should be addressed. E-mail: hwitek@mail.nctu.edu.tw.

10.1021/jp070786o CCC: $37.00 © 2007 American Chemical Society
Published on Web 06/14/2007

Similarly, harmonic vibrational frequencies calculated with the SCC−DFTB method are of similar quality like DFT if one uses specially reoptimized parameter files.[13]

The most serious practical drawback of the SCC−DFTB method is its restricted applicability due to the limited number of existing parameter files. These so-called Slater−Koster parameter files contain all necessary integrals, precomputed for a large number of interatomic distances, together with one-center DFTB parameters and distance-dependent repulsive potentials. In the DFTB method, the Slater−Koster files play a dominant role comparable to the role of pseudopotentials and basis sets in DFT. However, in contrast to one-particle pseudopotentials or basis sets, the Slater−Koster parameter files are precomputed for pairs of atoms. Therefore, the parametrization effort of the DFTB method scales quadratically with the number of atomic species when compared to linear scaling for conventional DFT pseudopotential/basis set approaches. At present, the existing DFTB parameters cover mostly the first and second row of the periodic table, especially the elements C, O, N, F, H, and Si.[18]

A serious limitation of the existing parametrization program employed until now for calculating the Slater-Koster integrals is the use of the nonrelativistic Schrödinger equation to generate the atomic reference data, atomic potentials, and atomic wave functions. In the present study, we introduce a new DFTB parametrization paradigm that is based on numerical solutions of atomic Dirac−Kohn−Sham equations. This framework allows for including relativistic effects, both scalar and spin−orbit, in the parametrization process; it also enables us to treat all chemical elements, both light and heavy, on the same footing. For the lighter elements, the solutions of the Dirac equation tend to converge toward the solutions of the Schrödinger equation. This assures that the new DFTB parametrization scheme would yield similar results for light atoms like the parametrization based on the Schrödinger equation. This is a very important issue since the existing parameter sets for carbon, nitrogen, oxygen, and hydrogen have been extensively tested and are known to produce reliable molecular geometries and reaction energies.

At this point, we would like to note that a relativistic program to generate the Slater−Koster data needed by the DFTB program based on work by Seifert and Eschrig already exists.[19,20] However, it has severe technical limitations making it difficult to use in connection with the SCC−DFTB ansatz as developed by Elstner and co-workers.[11]

The organization of this paper is as follows. Section II gives a general outline of the parametrization process. Section III presents technical details of obtaining confined four-component atomic wave functions. Here, we discuss the theoretical formalism and describe the employed techniques and approximations. This section also presents a number of numerical results obtained with the new formalism. Section IV explains the details of obtaining one-component orbitals. The determination of Hubbard parameters is discussed in section V. The conclusions are given in section VI.

II. Relativistic SCC−DFTB Parametrization: An Overview

Determination of electronic DFTB parameters requires calculating the following quantities: (i) one-center valence orbitals energies, (ii) two-center overlap integrals at various internuclear distances, (iii) two-center Hamiltonian integrals at various internuclear distances, (iv) one-center Hubbard parameters, and (v) one-center spin-polarization constants. The one-center quantities are obtained by solving the atomic self-consistent-field (SCF) Dirac−Kohn−Sham problem. The two-center quantities can then be computed numerically as integrals over the valence atomic orbitals. Below we describe technical details of the first step of this process, determination of atomic wave functions, their energies, and the corresponding Hubbard parameters. Determination of the remaining components of Slater−Koster parameter files, i.e., spin-polarization constants, overlap and Hamiltonian integrals, and two-center repulsive potentials, will be presented in subsequent publications. Some of the technical details given in this article have been already presented in various monographs; however, we find it appropriate to collect all of this scattered information here in one place so that they can serve in a twofold manner: as a complete reference for the relativistic parametrization of DFTB and as an instructive manual for the DFTB parametrization program (especially with respect to the information presented in the Supporting Information).

We have decided to choose the Dirac equation in our parametrization process to provide a consistent physical framework for all atoms through the periodic table of elements. This choice ensures that relativistic effects are intrinsically included in the formalism. We would like to stress here that DFTB is essentially a nonrelativistic theory. The molecular eigenvalue problem is solved in a basis of one-component valence-shell atomic orbitals, and a nonrelativistic version of the molecular Hamiltonian operator is used to calculate the off-diagonal elements of the Hamiltonian matrix. [The off-diagonal elements of Hamiltonian can be in principle, calculated using also a relativistic form of kinetic energy operator, however the difference for valence shell electrons should be negligible.] The only places where relativity enters into the DFTB formalism then are (i) construction of a minimal atomic valence orbital basis, (ii) computing atomic densities (or alternatively atomic exchange-correlation potentials) used to construct the molecular exchange-correlation potential, and (iii) computing one-electron parameters like orbital energies and Hubbard parameters. The diagonal elements of the Hamiltonian matrix, i.e., orbital energies, are computed by appropriate averaging of spinor energies. The one-electron valence basis is a standard one-component basis obtained by neglecting the small components and appropriate averaging of the large components of valence spinors. The details of its construction are described below. The valence basis sets obtained in that way can be compared to basis sets obtained with the scalar portion of a two-component similarity-transformed Dirac operator. Some of the advantages of our approach are (i) atomic spinors are obtained as numerical solutions of differential equations, i.e., they correspond to a complete basis set limit, and (ii) the electron density obtained from our calculations contains also the spin−orbit effects.

III. One-Particle Spinor Energies and Wave Functions of Atoms

A. Method. The first stage of the parametrization process consists of solving radial Dirac−Kohn−Sham equations for a confined pseudoatom. Numerical solutions are computed using a modified Dirac−Slater program originally written by Desclaux.[21,22] Atomic four-component spinors ϕ_j are obtained by solving iteratively a system of coupled equations

$$[-ic\boldsymbol{\alpha}\nabla + (\beta - \mathbf{1})c^2 + v_{\text{eff}}]\phi_j = \epsilon_j\phi_j \qquad (3.1)$$

where ϵ_j denotes the energy of the jth spinor (without the rest energy mc^2), c is the velocity of light (which was taken to be 137.03599911), $\mathbf{1}$ denotes the 4×4 unit matrix, v_{eff} is an

effective potential, and α and β are Dirac matrices. All quantities are expressed in atomic units. The four-component spinor ϕ_j is given by

$$\phi_j = \frac{1}{r}\begin{pmatrix} P_j(r)\chi_\kappa^m \\ iQ_j(r)\chi_{-\kappa}^m \end{pmatrix} \tag{3.2}$$

where χ_κ^m and $\chi_{-\kappa}^m$ are two-component spinors obtained by appropriate combination of spherical harmonics multiplied by spin eigenfunctions $\binom{1}{0}$ and $\binom{0}{1}$. Owing to the spherical symmetry of the atomic problem, eq 3.1 can be reduced to a system of coupled differential equations for the large and small component radial functions $P_j(r)$ and $Q_j(r)$ of each spinor ϕ_j given by

$$\begin{cases} \dfrac{dP_j(r)}{dr} + \kappa\dfrac{P_j(r)}{r} + \left(-2c - \dfrac{\epsilon_j - v_{\text{eff}}}{c}\right) Q_j(r) = 0 \\ \dfrac{dQ_j(r)}{dr} - \kappa\dfrac{Q_j(r)}{r} + \left(\dfrac{\epsilon_j - v_{\text{eff}}}{c}\right) P_j(r) = 0 \end{cases} \tag{3.3}$$

where κ is the relativistic quantum number defined by the angular momentum quantum number l and the total momentum quantum number j as

$$\kappa = l(l+1) - \left(j + \frac{1}{2}\right)^2 \tag{3.4}$$

After introducing a new variable $t = \ln r$, eq 3.3 is transformed into

$$\begin{cases} \dfrac{dP_j(t)}{dt} + \kappa P_j(t) + e^t \left(-2c - \dfrac{\epsilon_j - v_{\text{eff}}}{c}\right) Q_j(t) = 0 \\ \dfrac{dQ_j(t)}{dt} - \kappa Q_j(t) + e^t \left(\dfrac{\epsilon_j - v_{\text{eff}}}{c}\right) P_j(t) = 0 \end{cases} \tag{3.5}$$

which is more suitable for numerical integration. This form assures finer integration mesh at the region close to the nucleus, i.e., in the region where the wave function changes rapidly. The effective potential v_{eff} is defined as

$$v_{\text{eff}} = v_{\text{nuc}} + v_{\text{Coul}} + v_{\text{xc}} + v_{\text{conf}} \tag{3.6}$$

where v_{nuc} is the nuclear attraction potential, v_{Coul} is the Coulomb potential, v_{xc} is an exchange-correlation potential, and v_{conf} is an additional confining potential. The first two components of the effective radial potential are given by

$$v_{\text{nuc}}(r) = -\frac{Z}{r} \tag{3.7}$$

$$v_{\text{Coul}}(r) = \frac{1}{r}\int_0^r \rho(r')\,dr' + \int_r^\infty \rho(r')\frac{dr'}{r'} \tag{3.8}$$

where Z is the nuclear charge. The radial electron density $\rho(r)$ is given by

$$\rho(r) = \frac{1}{r^2}\sum_j n_j(P_j^2 + Q_j^2) \tag{3.9}$$

where the summation runs over all occupied spinors and n_j denotes the occupation number of the spinor ϕ_j.

The $X\alpha$ exchange potential[23] of Slater, that was used in the original program of Desclaux,[21,22] is replaced by a more accurate exchange-correlation potential. In the present implementation, we are using as v_{xc} the nonrelativistic versions of LDA and GGA exchange-correlation potentials.[2,24,25] In general, we should employ a truly relativistic exchange-correlation potential that contains other physical effects in addition to the statistical and Coulomb correlations of the nonrelativistic formalism, e.g., retardation effects, magnetic interaction between electrons, vacuum polarization, and radiative corrections. Various versions of such relativistic exchange-correlation potentials have been proposed in the literature.[26−30] Here we have decided for the nonrelativistic form of v_{xc} since it is not obvious that these effects would be noticeable within the inherently approximate DFTB formalism.

B. Confining Potential. In standard ab initio methods, the atomic basis set is usually constructed as a linear combination of a large number of primitive functions with coefficients and exponents optimized for a free atom. However, if the optimization is performed for an atom in a molecule, the optimal values of the coefficients and exponents would be different. This problem arises from using an incomplete basis set to describe one-particle eigenstates of electrons in the atom. Such an inconvenient situation can be partially remedied by including in the atomic basis sets diffuse virtual orbitals. These additional orbitals provide extra variational freedom to readjust the linear combination coefficients of valence orbitals in a molecule. Unfortunately, such a solution cannot be used for the DFTB method while retaining its efficiency resulting from the use of a minimal valence basis set. Therefore, an additional radial confining potential $v_{\text{conf}}(r)$ is used in eq 3.6 to mimic the environment of atoms in solids and molecules.[31] The functional form of $v_{\text{conf}}(r)$ used in the previous nonrelativistic parametrization of DFTB was

$$v_{\text{conf}}(r) = \left(\frac{r}{r_0}\right)^k \tag{3.10}$$

where r_0 and k are variational parameters. (In practice k was very often set to 2 or 4 that left only one variational parameter, r_0.) This approach allowed for reducing the effective size of atoms by compressing the outer part of the electron density without changing its behavior in the core region. Unfortunately, this approach cannot be directly extended to the relativistic parametrization process. The potential given by eq 10 diverges for $r \rightarrow \infty$ yielding highly oscillatory asymptotic limits for P and Q given by

$$\begin{cases} P(r) \rightarrow b_1 \cos\left(\dfrac{r^{k+1}}{(k+1){r_0}^k}\right) + b_2 \sin\left(\dfrac{r^{k+1}}{(k+1){r_0}^k}\right) \\ Q(r) \rightarrow -b_2 \cos\left(\dfrac{r^{k+1}}{(k+1){r_0}^k}\right) + b_1 \sin\left(\dfrac{r^{k+1}}{(k+1){r_0}^k}\right) \end{cases} \tag{3.11}$$

These functions violate the usual boundary conditions inferred for bound states ($P(r)$, $Q(r) \rightarrow 0$ for $r \rightarrow \infty$) and give no restriction on permitted energy values. They are, however, permissible solutions for continuum states. Hence, the confining potential given by eq 3.10 produces a Dirac pseudo-atom with continuous energy spectrum that is of little use for the DFTB parametrization process. This situation has close analogy in the relativistic harmonic oscillator model[32,33] that also possesses a continuous energy spectrum. These two facts are in strong opposition to the nonrelativistic case and can be considered as a manifestation of the Klein paradox.[34]

This problem can be circumvented[35] by introducing a mixed, scalar−vector coupling for the confining potential. [We would like to thank the anonymous referee of this paper for bringing these results to our attention.] The resultant operator,

$[(1 + \beta)/2]v_{conf}(r)$, can be considered as a linear combination of a Lorentz scalar and time-like Lorentz vector potentials. Since such a confining potential acts only on the large component of every valence spinor, eq 3.1 can be reduced to a system of coupled differential equations for the components $P_j(r)$ and $Q_j(r)$ that is given by

$$\begin{cases} \dfrac{dP_j(r)}{dr} + \kappa\dfrac{P_j(r)}{r} + \left(-2c - \dfrac{\epsilon_j - v_{nuc} - v_{Coul} - v_{xc}}{c}\right) Q_j(r) = 0 \\ \dfrac{dQ_j(r)}{dr} - \kappa\dfrac{Q_j(r)}{r} + \left(\dfrac{\epsilon_j - v_{nuc} - v_{Coul} - v_{xc} - v_{conf}}{c}\right) P_j(r) = 0 \end{cases} \quad (3.12)$$

Solutions to this system of equations can be found using a numerical integration algorithm that is discussed in the next section of this article. The only required modification for solving eq 3.12, in comparison with our standard approach given by eq 3.3, concerns using a set of two effective radial potentials for each component of the spinor, $P_j(r)$ and $Q_j(r)$, that include or exclude, respectively, the additional confining potential.

In the present study, we introduce an alternative approach based on a confining potential that is coupled as a time-like component of a Lorentz four-vector. Such a choice seems to be more natural than that of Eschrig and co-workers[35] since the additional confining potential has then the same Lorentz transformation properties as the other components of the Hamiltonian. A proper radial confining potential that would be applicable in the relativistic four-component atomic calculations should fulfill a number of conditions. Such conditions were studied by Plesset[36] and Rose and Newton[37] for a family of central fields. They can be succinctly characterized by requiring that the only two singular points of differential equations given by eq 3.3, i.e., $r = 0$ and $r = \infty$, should be regular. In practice this means that the potential v_{eff} should fulfill two conditions: (i) $|\lim_{r\to 0}(rv_{eff})| \le 1$ and (ii) $|v_{eff}(\infty)| < \infty$. On the other hand, we require that the confining potential v_{conf} is negligible in the region corresponding to the atomic core and that it grows fast at the region outside the atomic radius. Motivated by these requirements, we have decided to employ in our parametrization scheme of DFTB the spherical Woods−Saxon potential[38,39] commonly used in nuclear theory. It is given by

$$v_{conf}(r) = \frac{W}{1 + e^{-a(r-r_0)}} \quad (3.13)$$

The values of a, r_0, and W in eq 3.13 can be optimized to provide a good representation of the electronic states in various molecules and solids. Intuitively, the value of r_0 should be similar to the atomic radius and a should be larger than 2 to ensure the unperturbed character of ρ in the atomic core region.

Both approaches, the Woods−Saxon potential and the relativistic generalization[35] of the confining potential of Eschrig and co-workers,[31,40] have been included as options in our parametrization program. The Woods−Saxon confining potential seems to provide more variational freedom than the potential suggested by Eschrig and co-workers.[35] This additional freedom can be used for more efficient fine-tuning of atomic densities and orbitals in order to reproduce accurately various molecular and solid-state properties. The Woods−Saxon potential yields correct $\exp(-\alpha r)$ asymptotics of atomic orbitals, whereas the orbitals obtained with the $(r/r_0)^k$ potential vanish faster with the $\exp(-\alpha r^{1+k/2})$ asymptotics. Another favorable feature of the Woods−Saxon confining potential is its noninvasive character in the atomic core region, since an appropriate choice of large a in eq 3.13 gives a potential that closely resembles a square well with smooth walls. On other hand, an advantage of the family of the $(r/r_0)^k$ confining potentials is their well studied behavior, both in nonrelativistic and relativistic framework. Several other forms of admissible potentials have been suggested for the radial Dirac equation in the literature.[41−43] We believe that inclusion of the two particular forms of confining potentials described above is sufficient for a successful parametrization of DFTB. Numerical tests of the new approach that uses the Woods−Saxon confining potential are discussed below.

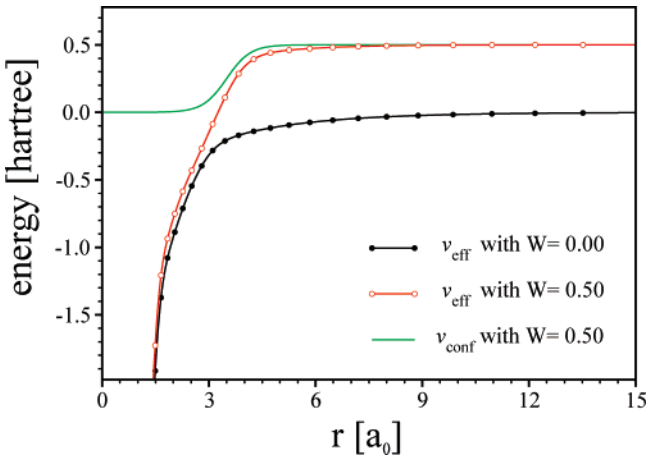

Figure 1. Effective radial potential v_{eff} calculated for the lead atom in the presence ($W = 0.50$) or absence ($W = 0.00$) of the additional confining Woods−Saxon potential. The shape of the confining potential v_{conf} is shown for comparison.

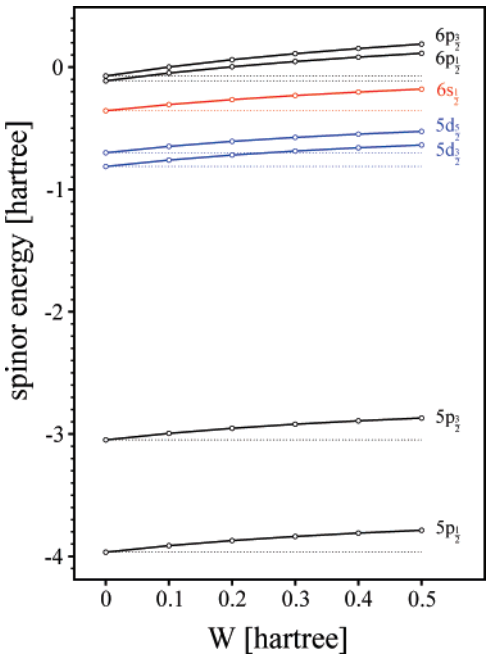

Figure 2. Dependence of one-particle spinor energies of lead on the height W of the confining Woods−Saxon potential.

Figure 1 gives a comparison of total effective potential v_{eff} obtained for the lead atom with and without the Woods−Saxon confining potential given by eq 3.13. For completeness, we also show the shape of the confining potential v_{conf} in which the following parameters have been used: $a = 3$, $r_0 = 3.5$ (which is approximately equal to the atomic radius of lead), and $W = 0.5$ hartree. The effect of the applied confining potential on the one-particle atomic energies is shown in Figure 2. We plot there the spinor energies against the height of the confining potential

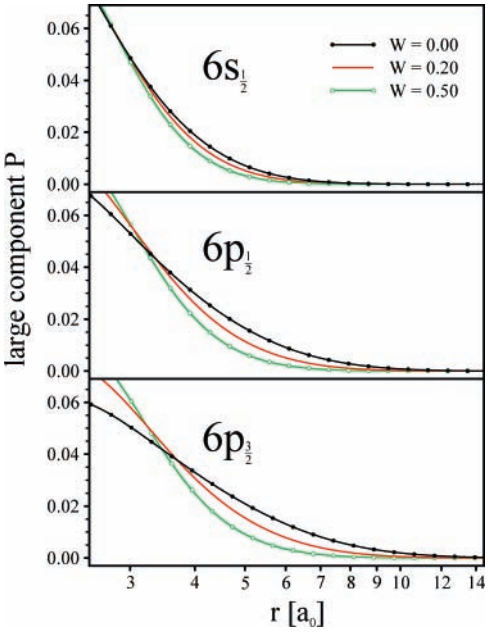

Figure 3. Contraction of the large component radial function P of the $6s_{1/2}$, $6p_{1/2}$, and $6p_{3/2}$ spinors of lead in the valence region. The wave functions have been calculated with three different values of W (W = 0.00, 0.20, and 0.50) defining the confining Woods−Saxon potential.

W, which varies smoothly in the range between 0.0 and 0.5 hartree. As expected, the values of ϵ_j grow monotonically with increasing W. This behavior can be anticipated from Figure 1, where the effective potential well is "narrower" with the confining potential switched on. The effect of the applied confining potential on the shape of valence wave functions is shown in Figure 3. This figure shows the change in the tail region of the large component P of the 6s, $6p_{1/2}$, and $6p_{3/2}$ spinors of lead for three different values of W: 0.0, 0.2, and 0.5 hartree. To visualize better the changes over a large range of distances, we choose to plot the abscissa values on the logarithmic scale. It can be seen that the larger value of W yields more compact wave functions, which justifies the name of the confining potential. In addition to the information presented in Figure 3, we would like to emphasize another two facts concerning the confined wave functions: (i) the nodal points of confined and pristine wave functions are approximately identical and (ii) the shape of wave function obtained for the core spinors is identical with the confining potential switched on or off. Both these facts are readily understandable if one realizes that the confining potential is negligible in the atomic core region, i.e., the region responsible for the shape of inner spinors and the region where most of wave function nodes are located. Very similar features can be also observed for atomic radial densities. Figure 4 shows radial electron densities calculated for carbon, germanium, and lead with and without the confining potential. We have used the following values of a and r_0 in our calculations: $a = 6$ and $r_0 = 1.3$ for carbon, $a = 4$ and $r_0 = 2.4$ for germanium, and $a = 3$ and $r_0 = 3.5$ for lead. The employed values of W are specified in the Figure 4. All values are given in atomic units.

C. Technical Details. Solutions of a set of differential equations of first-order given by eq 3.5 are obtained with a five-step Adams predictor-corrector method. Technical details[44,45] concerning this approach are given in the Supporting Information. This integration technique provides a stable computational algorithm except for the regions where $P_j(t)$ and $Q_j(t)$ have approximately exponential character, i.e., at regions where $t \rightarrow 0$ and $t \rightarrow \infty$. To avoid numerical instabilities in these regions, the step-by-step integration must proceed in the direction in which the solution sought is increasing. We therefore require outward integration for small t and inward integration for large t, together with some procedure for matching the two solutions at some convenient intermediate point.[46] In the present implementation, we follow Desclaux[44,21,22] and choose for this purpose the outer classical turning point determined for the corresponding nonrelativistic limit of eq 3.5 given by

$$\frac{1}{2}\frac{d^2P_j}{dr^2} - \left(\frac{\kappa(\kappa+1)}{2r^2} - \epsilon_j + v_{\text{eff}}(r)\right)P_j = 0 \qquad (3.14)$$

i.e., the point $t_k = \ln r_k$, for which

$$\frac{\kappa(\kappa+1)}{2r_k^{\,2}} + v_{\text{eff}}(r_k) = \epsilon_j \qquad (3.15)$$

The selected integration algorithm requires knowing the values of P_j and Q_j at five consecutive points of the mesh to start out the integration process. The initial conditions for the outward integrations are obtained through a series expansion of P_j and Q_j around the origin

$$\begin{aligned} P_j(r) &= r^{\gamma}(p_0 + p_1 r + p_2 r^2 + p_3 r^3 + \dots) \\ Q_j(r) &= r^{\gamma}(q_0 + q_1 r + q_2 r^2 + q_3 r^3 + \dots) \end{aligned} \qquad (3.16)$$

The value of γ can be found after substituting eq 3.16 into eq 3.3 and taking the limit $r \rightarrow 0$. It is given by

$$\gamma = \sqrt{\kappa^2 - \frac{Z^2}{c^2}} \qquad (3.17)$$

This limit yields also the relationship between p_0 and q_0; it is given by

$$p_0 = \frac{(\kappa - \gamma)c}{Z} q_0 \qquad (3.18)$$

Higher coefficients appearing in eq 3.16 can be found in a similar manner. Their detailed derivation is given in many textbooks (we give this derivation in the Supporting Information for the completeness of this presentation together with the derivation of initial conditions for the inward integration); p_l and q_l for $l = 1, 2, 3, \dots$ are given recursively by

$$\begin{aligned} p_l &= \frac{(l+\gamma-\kappa)(2c-w)}{l(l+2\gamma)}\, q_{l-1} + \frac{Z}{c}\frac{w}{l(l+2\gamma)}\, p_{l-1} \\ q_l &= \frac{(l+\gamma+\kappa)w}{l(l+2\gamma)}\, p_{l-1} - \frac{Z}{c}\frac{2c-w}{l(l+2\gamma)}\, q_{l-1} \end{aligned} \qquad (3.19)$$

where w is related to the slowly varying part of the potential and is computed at the first grid point r_1 of the mesh as

$$w = \frac{1}{c}[v_{\text{Coul}}(r_1) + v_{\text{xc}}(r_1) + v_{\text{conf}}(r_1) - \epsilon] \qquad (3.20)$$

The series given by eq 3.16 converges fast for small r giving initial conditions for the outward integration. The value of q_0 is taken to be ± 1 with a sign assuring that the large component radial function P is positive for large values of r. The initial conditions for the inward integration are obtained by inspecting

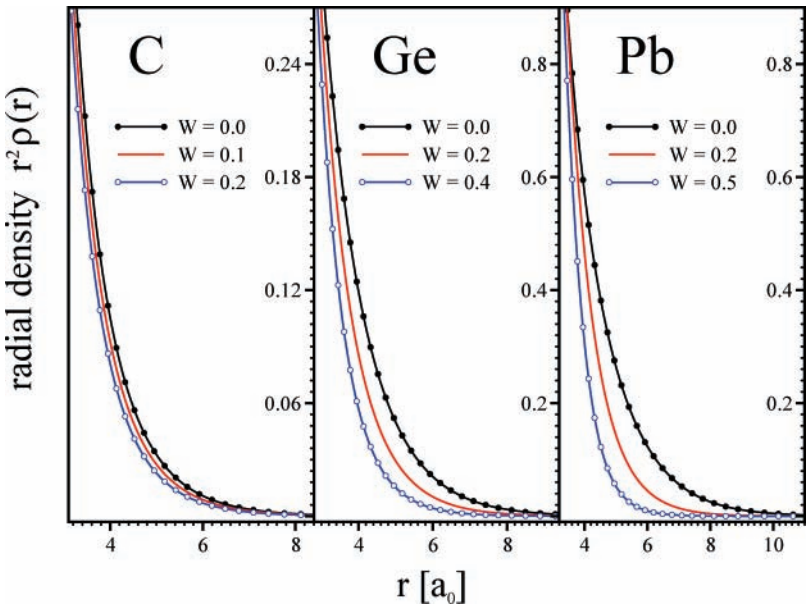

Figure 4. Contraction of the radial electron density of carbon, germanium, and lead in the valence region. The densities have been calculated with three different values of W defining the confining Woods−Saxon potential.

the solutions of a set of differential equations obtained from eq 3.3 for $r \rightarrow \infty$. They are given by

$$P(r) = b \exp\left[-\left(\sqrt{-2(\epsilon - W) - \frac{(\epsilon - W)^2}{c^2}}\right)r\right] \quad (3.21)$$

and

$$Q(r) = -\sqrt{\frac{-\epsilon + W}{2c^2 + \epsilon - W}}P(r) \quad (3.22)$$

where W is the limit of v_{eff} at large distance and b is an adjustable constant. In the case when the relativistic generalization of the confining potential $(r/r_0)^k$ of Eschrig and co-workers is employed instead of the Woods−Saxon potential, the initial conditions for the inward integration are given by

$$P(r) = br^{-(k/4)} \exp\left(-\frac{2(2c^2 + \epsilon)}{(k+2)c^2 r_0^{\,k}} r^{(k+2)/2}\right) \quad (3.23)$$

and

$$Q(r) = -\sqrt{\frac{1}{(2c^2 + \epsilon)r_0^{\,k}}} r^{(k/2)} P(r) \quad (3.24)$$

where b is an adjustable constant. Derivation of these equations is given in the Supporting Information.

The outward integration is performed from the origin to the classical turning point. If the number of nodal points is wrong, the value of spinor energy ϵ is adjusted and the integration is repeated. After assuring proper number of nodes in the outward integration region, the inward integration is performed. The values of the large component radial function at the classical turning point obtained from both integration procedures are matched, $P(r_k^+) = P(r_k^-)$, by appropriate choice of b in eq 3.21. Similar matching of values of the small component radial function, $Q(r_k^+) = Q(r_k^-)$, can be only achieved if the wave functions are evaluated with the correct energy eigenvalue ϵ. The attempt to match the small component yields[47] a correction to the energy eigenvalue equal to

$$\Delta\epsilon = \frac{cP(r_k)(Q(r_k^+) - Q(r_k^-))}{\int_0^\infty (P^2(r) + Q^2(r))\,\mathrm{d}r} \quad (3.25)$$

After the modification of the spinor energy ϵ, the procedure of outward and inward integration is restarted and the iterations are continued until convergence is achieved.

IV. Scalar Relativistic One-Particle Orbital Energies and Wave Functions of Atoms

Relativistic atomic spinor radial wave functions are characterized by the quantum numbers n and κ. Scalar relativistic atomic orbital radial wave functions are characterized by the quantum numbers n and l. The latter can be obtained directly by solving an equation analogous to eq 3.3 but without the spin−orbit coupling terms. Here we adopt another approach[20] following Heera, Seifert, and Ziesche. We simply average the spin−orbit split components of p, d, and f orbitals using the following formula:

$$\begin{pmatrix} P_l \\ Q_l \end{pmatrix} = \frac{l}{2l+1}\begin{pmatrix} P_{\kappa=l} \\ Q_{\kappa=l} \end{pmatrix} + \frac{l+1}{2l+1}\begin{pmatrix} P_{\kappa=-l-1} \\ Q_{\kappa=-l-1} \end{pmatrix} \quad (4.1)$$

Orbital energies are obtained using a similar formula

$$\epsilon_l = \frac{l}{2l+1}\epsilon_{\kappa=l} + \frac{l+1}{2l+1}\epsilon_{\kappa=-l-1} \quad (4.2)$$

It must be stressed that the relativistic orbitals obtained from such averaged radial wave functions neglect completely the spin−orbit coupling effects.

For the purpose of parametrization of DFTB, we need one-component orbitals for each atomic valence subshell. We obtain them by neglecting the small radial component $Q_l(r)$ in the orbital given by eq 4.1. Note that this procedure is a good approximation since for the valence spinors the value of the small component is usually much smaller than the value of the

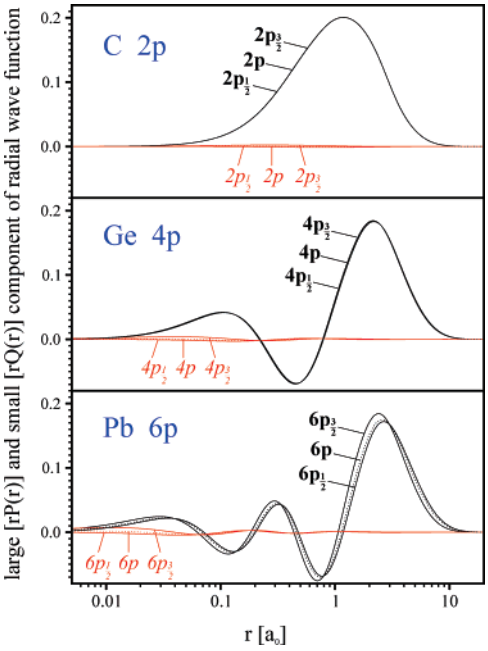

Figure 5. Plots of large (bold characters) and small (slant characters) components of the atomic spinor (solid line) and orbital (dotted line) radial wave functions for the 2p shell of carbon, the 4p shell of germanium, and the 6p shell of lead. For carbon and germanium, the large component of the orbital radial wave function and its both spin−orbit split constituents almost coincide.

large component. This is especially true for the region outside the atomic core. (See the relationship between $P(r)$ and $Q(r)$ given by eqs 3.22 and 3.18.) A formal justification of neglecting the small component was given[20] by Heera, Seifert, and Ziesche. Numerical examples of this procedure are given in Figure 5, which shows the large and small components of the 2p orbital of carbon, the 4p orbital of germanium, and the 6p orbital of lead together with the corresponding spin−orbit split spinor wave functions. For carbon and germanium, the spin−orbit split spinor components are practically identical, especially for the large component radial wave functions. For lead, the differences are more distinct, but the overall shape and characteristics of both spinor wave functions are very similar. The small component wave functions are almost negligible in comparison with the large component wave functions. The presented results suggest that both approximations, averaging spin−orbit split portions of the large component and neglecting entirely the small component, are legitimate.

The final valence orbitals used in the DFTB parametrization then have the following form:

$$\psi_{nlm}(r, \theta, \phi) = P_{nl}(r)Y_l^m(\theta, \phi) \tag{4.3}$$

where $P_{nl}(r)$ denotes the radial wave function obtained from eq 4.1 and $Y_l^m(\theta, \phi)$, usual spherical harmonics. The radial wave functions $P_{nl}(r)$ are obtained as a collection of values at the grid points. To obtain a convenient analytical representation of $P_{nl}(r)$ a fit is performed using cubic spline functions. A similar fitting procedure is applied to atomic density ρ and atomic exchange-correlation potential v_{xc} to provide an analytical representation of these quantities to be used in the further steps of the parametrization process.

V. Atomic Hubbard Parameters

In the nonrelativistic case, we define the Hubbard parameter U_{Al} for the orbital l of atom A by the derivative

$$U_{Al} = \frac{\partial \epsilon_l}{\partial n_l} \tag{5.1}$$

Here ϵ_l is the Kohn−Sham single particle energy of orbital l and n_l is its (noninteger) occupation number. Obviously, owing to self-consistency requirements, one has to address this equation by a numerical differentiation scheme. The Hubbard parameters U are then used in the SCC−DFTB calculations to evaluate the energy change due to charge redistribution, either between atoms or between various atomic angular shells.

Retaining the fundamental design of the SCC−DFTB energy expression, one has to translate the procedure defined by eq 5.1 to the framework of the relativistic Dirac−Kohn−Sham problem. To this end, we have to express eq 5.1 using quantities available from the relativistic treatment. The ϵ_l can be replaced by a linear combination of spinor single particle energies according to eq 4.2. Similarly, the nonrelativistic occupation number n_l can be expressed as a some linear combination of the spinor occupation numbers. Both quantities can be substituted to eq 5.1 to yield its relativistic equivalent.

However, for the numerical differentiation, one has to distribute a finite change in n_l to the spinor occupation numbers. It is not obvious how this has to be done. For example one could distribute this linearly or using the same weights as are used in eqs 4.1 and 4.2. An alternative approach is to average the spinor Hubbard parameters $U_{A\kappa}$ with the same weights as in eq 4.2. The Hubbard parameters $U_{A\kappa}$ can be obtained with a relativistic analog of eq 5.1 given by

$$U_{A\kappa} = \frac{\partial \epsilon_\kappa}{\partial n_\kappa} \tag{5.2}$$

Table 1 presents the values of Hubbard parameters U calculated for the 2p orbitals of carbon and the 5d and 6p orbitals of lead. These values have been obtained using both approaches, by averaging appropriate spinor Hubbard parameters $U_{A\kappa}$, and by weighted scaling of appropriate spinor occupation numbers n_κ. We denote these values respectively by U_{aver} and U_{scal}. The presented results show that the values of U_{Al} do not depend on the procedure used for their determination; the numerical values of U_{aver} and U_{scal} computed for carbon and lead are identical. For future reference, we decide to obtain the values of U_{Al} by averaging appropriate spinor Hubbard parameters $U_{A\kappa}$. The entries in Table 1 have been obtained with the LDA exchange-correlation functional and with no confining potential. The two electrons in the valence p orbitals have been distributed to the

TABLE 1: Values of the Hubbard Parameters Calculated for the 2p Orbitals of Carbon and the 5d and 6p Orbitals of Lead[a]

C, 2p Orbitals			
$U(2p_{1/2})$	$U(2p_{3/2})$	$U(2p)_{\text{aver}}$	$U(2p)_{\text{scal}}$
0.381	0.381	0.381	0.381
Pb, 6p Orbitals			
$U(6p_{1/2})$	$U(6p_{3/2})$	$U(6p)_{\text{aver}}$	$U(6p)_{\text{scal}}$
0.208	0.181	0.190	0.190
Pb, 5d Orbitals			
$U(5d_{3/2})$	$U(5d_{5/2})$	$U(5d)_{\text{aver}}$	$U(5d)_{\text{scal}}$
0.420	0.409	0.413	0.413

[a] For details, see the text.

corresponding spinors $p_{1/2}$ and $p_{3/2}$ in proportion 1:2 giving fractional spinor occupations 2/3 and 4/3; analogous procedure is applied for the d orbitals.

VI. Conclusion

We have presented an extensive treatment of a confined relativistic atom as it applies to the DFTB method. Explicit formulas for obtaining wave functions, on-site orbital energies, Hubbard *U* parameters, and atomic potentials and densities have been presented. Two different versions of the radial confining potential applicable to the relativistic four-component Dirac−Kohn−Sham problem have been discussed and implemented in the parametrization program: (i) relativistic version of quartic potential of Eschrig and co-workers and (ii) the Woods−Saxon potential. The effect of the additional confinement on the energy eigenvalues and the shape of atomic wave functions and densities is studied for the Woods−Saxon potential and numerical examples are presented for the valence spinors of carbon and lead. An approximate averaging technique is employed for determining one-component orbitals from the four-component spinors. The presented numerical results for the 2p shell of carbon, the 4p shell of germanium, and the 6p shell of lead show that the averaging of large components and neglecting small components is a legitimate approximation for valence shell spinors.

Acknowledgment. We thank Dr. Uwe Gerstmann for the initial version of the atomic code by J. P. Desclaux. H.A.W. acknowledges the National Science Council of Taiwan for financial support (NSC 95-2113-M-009-016). This research has also been supported by Institute of Nuclear Energy Research, Atomic Energy Council, Taiwan, under Contract No. NL940251.

Supporting Information Available: Additional calculations. This material is available free of charge via the Internet at http://pubs.acs.org.

References and Notes

(1) Slater, J.; Koster, G. *Phys. Rev.* **1954**, *94*, 1498.
(2) Kohn, W.; Sham, L. *Phys. Rev.* **1965**, *140*, A1133.
(3) Hohenberg P.; Kohn, W. *Phys. Rev.* **1964**, *136*, B864.
(4) Eschrig, H. *The Fundamentals of Density Functional Theory*; Gutenbergplatz: Leipzig, Germany, 2003.
(5) Bieger, W.; Seifert, G.; Eschrig, H.; Grossmann, G. *Z. Phys. Chem. (Leipzig)* **1985**, *266*, 751.
(6) Seifert, G.; Eschrig, H.; Bieger, W. *Z. Phys. Chemie (Leipzig)* **1986**, *267*, 529.
(7) Blaudeck, P.; Frauenheim, T.; Porezag, D.; Seifert, G.; Fromm, E. *J. Phys.* **1992**, *4*, 6389.
(8) Porezag, D.; Frauenheim, T.; Köhler, T.; Seifert, G.; Kaschner, R. *Phys. Rev. B* **1995**, *51*, 12947.
(9) Harris, J. *Phys. Rev. B* **1985**, *31*, 1770.
(10) Foulkes, W.; Haydock, R. *Phys. Rev. B* **1989**, *39*, 12520.
(11) Elstner, M. et al., *Phys. Rev. B* **1998**, *58*, 7260.
(12) Krüger, T.; Elstner, M.; Schiffels, P.; Frauenheim, T. *J. Chem. Phys.* **2005**, *122*, 114110.
(13) Mołepsza, E.; Witek, H.; Morokuma, K. *Chem. Phys. Lett.* **2005**, *412*, 237.
(14) Witek, H.; Irle, S.; Morokuma, K. *J. Chem. Phys.* **2004**, *121*, 5163.
(15) Witek, H.; Morokuma, K. *J. Comput. Chem.* **2004**, *25*, 1858.
(16) Köhler, C.; Seifert, G.; Frauenheim, T. *Chem. Phys.* **2005**, *309*, 23.
(17) Frauenheim, T;. et al. *Phys. Stat. Sol. B* **2000**, *217*, 41.
(18) http://www.dftb.org.
(19) Hourahine, B.; Sanna, S.; Aradi, B.; Köhler, C.; Frauenheim, T. *Physica B* **2006**, *376*, 512.
(20) Heera, V.; Seifert, G.; Zeische, P. *J. Phys. B* **1984**, *17*, 519.
(21) Desclaux, J. *Comp. Phys. Commun.* **1969**, *1*, 216.
(22) Desclaux, J. *Comp. Phys. Commun.* **1975**, *9*, 31.
(23) Slater, J. *Phys. Rev.* **1951**, *81*, 385.
(24) Perdew, J.; Burke, K.; Ernzerhof, M. *Phys. Rev. Lett.* **1996**, *77*, 3865.
(25) Perdew, J.; Burke, K.; Ernzerhof, M. *Phys. Rev. Lett.* **1997**, *78*, 1396.
(26) MacDonald, A.; Vosko, S. *J. Phys. C* **1979**, *12*, 2977.
(27) Engel, E.; Keller, S.; Facco Bonetti, A.; Müller, H.; Dreizler, R. *Phys. Rev. A* **1995**, *52*, 2750.
(28) Engel, E.; Keller, S.; Dreizler, R. *Phys. Rev. A* **1996**, *53*, 1367.
(29) Mayer, M.; Häberlen, O.; Rösch, N. *Phys. Rev. A* **1996**, *54*, 4775.
(30) van Wüllen, C. *J. Comput. Chem.* **2002**, *23*, 779.
(31) Eschrig, H. *Optimized LCAO Method and the Electronic Structure of Extended Systems*; Springer: Berlin, 1989.
(32) Nikolsky, K. *Z. Phys.* **1930**, *62*, 677.
(33) Postepska, I. *Acta Phys. Pol.* **1935**, *4*, 269.
(34) Klein, O. *Z. Phys.* **1929**, *53*, 157.
(35) Eschrig, H.; Richter, M.; Opahle, I. Relativistic solid state calculations. In *Relativistic Electronic Structure Theory, Part 2: Applications*; Schwerdtfeger, P., Ed.; Elsevier: Amsterdam, 2004.
(36) Plesset, M. *Phys. Rev.* **1932**, *41*, 278.
(37) Rose M.; Newton, R. *Phys. Rev.* **1951**, *82*, 470.
(38) Woods, R.; Saxon, D. *Phys. Rev.* **1954**, *95*, 577.
(39) Kennedy, P. *J. Phys. A* **2002**, *35*, 689.
(40) Eschrig H.; Bergert, I. *Phys. Stat. Sol. B* **1978**, *90*, 621.
(41) Ciftci, H.; Hall, R.; Saad, N. *Phys. Rev. A* **2005**, *72*, 022101.
(42) Bose, S.; Schulze-Halberg, A.; Singh, M. *Phys. Lett. A* **2001**, *287*, 321.
(43) Micu, L. *Mod. Phys. Lett. A* **2003**, *18*, 2895.
(44) Desclaux, J.; Mayers, D.; O'Brien, F. *J. Phys. B* **1971**, *4*, 631.
(45) Zabloudil, J.; Hammerling, R.; Szunyogh, L.; Weinberger, P. *Electron scattering in solid matter*; Springer: Berlin, 2005.
(46) Mayers, D.; O'Brien, F. *J. Phys. B* **1968**, *1*, 145.
(47) Liberman, D.; Waber, J.; Cromer, D. *Phys. Rev.* **1965**, *137*, A27.